Correlation between gas-phase OH density and intensity of luminol chemiluminescence in liquid interacting with atmospheric-pressure plasma

Naoki Shirai
Hokkaido University, Japan
E-mail: nshirai@qe.eng.hokudai.ac.jp

Goju Suga
Hokkaido University, Japan
E-mail:

Koichi Sasaki
Hokkaido University, Japan
E-mail:

Abstract.
The relationship between the density of OH radicals in the gas phase and the intensity of luminol chemiluminescence was investigated using an atmospheric-pressure plasma system in contact with liquid. The luminol chemiluminescence with a thin thickness was observed just below the plasma-liquid interface when the plasma was generated on the aqueous solution surface with luminol. The radial region with the chemiluminescence was approximately 2.6 times larger than that of the plasma with the optical emission, and was similar to the diameter of the region with OH radicals in the gas phase. The decay time constant of the intensity of the luminol chemiluminescence in the afterglow phase of the pulsed discharge was approximately 100 μs, while the optical emission intensity at the second positive system of molecular nitrogen decayed immediately after the termination of the discharge current. On the other hand, the decay time constant of the OH radical density was approximately 100 μs in the afterglow phase. These experimental results indicate that the luminol chemiluminescence is induced by the transport of OH radicals to the plasma-liquid interface. It is considered that the chemiluminescence is originated by the reaction with O_2^- which is produced by $OH + H_2O_2 \rightarrow O_2^- + H_3O^+$.

PACS numbers: 52.50, 52.80, 78.60

1. Introduction

Atmospheric-pressure plasmas interacting with liquids have been focused by many authors in the last decade with the intention of applying them to various technologies

such as water treatment, material processing, and biomedical fields [1–3]. We reported the characteristics of an atmospheric-pressure dc glow discharge using a liquid electrode [4–11]. It is believed that the interfacial region between a liquid and a plasma is highly reactive. The interfacial region with high reactivity is thin (several micrometers or less), but the thin region contains high densities of short-lived reactive species locally, which induce various chemical reactions which are important in various applications. Hence the deep understanding on short-lived species in the interfacial region is important. However we have serious defficluty in the detection of short-lived species in the interfacial region.

In general, the detection of long-lived species is much easier than the detection of short-lived species, and optical absorption spectroscopy [12] and light-induced fluorescence [13] have been adopted to the detection of long-lived species. In contrast, the real-time detection of short-lived reactive species in liquids is a hard task even for analytical chemists. A method for detecting OH radicals, which is a typical short-lived radical in liquid, is using terephthalic acid (TA) as the chemical probe [14–16]. The reaction between OH and TA forms 2-hydroxyterephthalic acid (HTA), and HTA is detected by light-induced fluorescence. However, this method cannot be used for the real time detection of OH, since HTA has a long lifetime and is accumulated in the liquid.

In a previosu work, we reported the use of the chemiluminescence (CL) of luminol (3-aminophthalhydrazide) to detect short-lived reactive species which are induced in a liquid by the interaction with an atmospheric-pressure plasma [17]. It has been shown that the luminol CL has a quick response to the initiation and the termination of the discharge, suggesting its usefulness to the real-time detection of short-lived species. It is known that the luminol CL is observed when luminol reacts with O_2^- [18]. However, in the previous work, we observed the positive correlation between the intensity of the luminol CL and the amount of OH detected by the chemcal probe method using TA. This observation suggests the production of O_2^- from OH, and in this case the luminol CL is applicable to the detection of OH in the liquid.

In this work, we examined the correlation between the intensity of the luminol CL and the OH density in the gas phase. The objective of this work is to clarify the detection of liquid-phase OH radicals using the luminol CL. We compared the spatial distribution and the temporal variation of the OH radical density in the gas phase with those of the luminol CL.

2. Experimental procedure

Figure 1 shows the schematic of the discharge system, the system for measuring the OH radical density in the gas phase, and the system for detecting the luminol CL in the liquid. We employed aqueous solutions as the liquid in this experiment. The electrode configuration was similar to that employed in our previous works [4, 5, 17]. A metal nozzle having an inner diameter of 0.5 mm was used as an electrode, and a mixed aqueous solution of luminol (0.5 mM) and sodium hydroxide (0.1 M) worked as the other

electrode for the discharge. The electrical conductivity and the pH of the liquid were 20 mS/cm and 13, respectively. A high voltage, which was measured using a high-voltage probe, was applied between the nozzle electrode and the liquid to generate a plasma along the helium flow toward the liquid surface. The flow rate of helium was 200 ccm. The distance between the top of the nozzle electrode and the liquid surface was 1-3 mm. A platinum wire was immersed in the liquid to connect it to a resistor of 100 Ω, which was used for measuring the discharge current. To investigate the temporal variations of the OH density and the intensity of luminol CL, we used pulsed power supply with a rectangular waveform for the discharge. The pulsed voltage with an arbitrary duration was obtained by switching the dc high voltage using a fast semiconductor unit. The amplitude of the pulsed voltage after breakdwon was 500-1000 V. Typical waveforms of the discharge voltage and the discharge current are depicted in figure 1. The details of the electrical circuit is described in our another previous work [4].

We took the photograph of CL by watching it from the bottom through the transparent side wall of the liquid container using a CCD camera to examine the shape and the size of the region with CL. The camera lens was not UV-transparent. An example of the CL photograph is inserted in figure 1. The thickness of the region with CL has not been identified yet, but it may be thinner than 0.1 mm according to the photograph. We also measured the optical emission spectrum of CL by guiding it to a spectrograph using an optical fiber. A lens was used for projecting the CL image onto the input side of the optical fiber. The diameter of the region with CL was determined by inserting a ruler at the same position as CL and by taking its picture using the same CCD camera. The sensitivity of the spectrograph as a function of the wavelength was calibrated using a standard tungsten lamp. The temporal variations of the intensities of CL and optical emission from the plasma were measured using a multichannel scaler (Stanford Research Systems, SR430) and a monochromator (Ritu Oyo Kogaku, MC-10N) with a photomultipler tube (PMT) (Hamamatsu, R955). We chose 1 kΩ for the load resistor of PMT to realize the photon counting measurement. The number of electrical pulses from PMT, which represented photons transmitted through the monochromator, was counted using the multichannel scaler with a bin width of 320 ns.

To investigate the OH radical density in the gas phase, we used laser-induced fluorescence (LIF) imaging spectroscopy [8,9]. The light source in this experiment was an optical parametric oscillator (OPO)(Spectra Physics, Quanta-Ray MOPO-HF), which generated a tunable pulsed laser beam at a wavelength of 283.0 nm. The laser beam excited OH radicals from the ground state $[X^2\Pi(v''=0)]$ to an electronic excited state $[A^2\Sigma^+(v'=1)]$. The image of the fluorescences by the transitions from $A^2\Sigma^+(v'=1)$ to $X^2\Pi(v''=1)$ and from $A^2\Sigma^+(v'=0)$ to $X^2\Pi(v''=0)$ was captured using a CCD camera with a gated image intensifier (Princeton, PI-MAX4) combined with a UV-transparent lens (Nikon, UV-Nikkor). The $A^2\Sigma^+(v'=0)$ state was produced by the vibrational energy transfer from $A^2\Sigma^+(v'=1)$. The temporal variation of the OH density was obtained by changing the delay time between the termination of the discharge current

and the oscillation of the tunable laser pulse. Exposure time of ICCD camera was 100 ns. Note that we have to pay considerable attention to the influences of collisional quenching and rotational temperature to obtain an accurate distribution of the OH radical density [8]. However, in this experiment, we did not take care the collisional quenching and the rotational temperature. Hence the image of LIF obtained in this experiment gave us the rough representation of the distribution of the OH radical density.

3. Results

Figure 2 shows the CL spectrum induced by the plasma irradiation. The spectrum had a broad width with the peak at around 425 nm. The CL spectrum induced by the reaction between H_2O_2 and luminol in the presence of Fe^{3+} is also shown in figure 2 for comparison. This CL was obtained by introducing a potassium ferricyanide solution into a mixed solution of luminol and H_2O_2. This chemiluminescence is widely utilized in many experiments in food analyses [19], liquid analyses [20] and blood detection [21]. As shown in the figure, the CL spectra induced by the plasma and the reaction with H_2O_2 were almost identical. It is noted here that, as will be described in discussion, the CL spectrum induced by the reaction with H_2O_2 was reconstructed from the directly measured spectrum by considering the optical absorption spectrum of the potassium ferricyanide solution.

Figure 3 shows the photographs of the plasma and CL observed at various discharge currents. The liquid worked as the cathode and the distances between the tip of the nozzle electrode and the liquid surface were 1 and 3 mm. The photographs of the plasma were taken from the upper side of the plasma-liquid interface (or the gas-phase side), while the photographs of CL were taken from the liquid side. The size scales are almost the same in the photographs shown in figures. 3(a) and 3(b). As reported in previous papers [4,5,8,9], we observed the Na D line (583 nm) in the gas phase when the liquid worked as the cathode of the discharge at discharge currents higher than 20 mA. As shown in figure 3(a), we observed the radial expansion of the region with the optical emission with the increase in the discharge current. The diameter of the region with CL in the liquid also expanded with the discharge current as shown in figure 3(b). However, as shown in the figure, the region with CL was always wider than the region with the optical emission of the plasma, and CL was observed even in the outside region of the Na D line. In addition, the shape of CL was dependent on the distance between the tip of the needle electrode and the solution surface. The shapes of CL were rings when the distance was 1 mm, as shown in figure 3(b), while we observed disks for the shapes of CL when the distance was 3 mm.

Figure 4 shows the distribution of the optical emission intensity of the plasma (figure 4(a)), which was observed using the ICCD camera, together with the LIF image of OH radicals (figure 4(b)). The liquid worked as the cathode and the distance between the tip of the nozzle electrode and the liquid surface was 3 mm. The discharge current

was 60 mA. The diameter of the plasma with the optical emission was approximately 1.0 mm. Figure 4(c) shows the photograph of CL which was obtained by placing a blue filter which eliminated the optical emission of Na. The shape of CL was a uniform disk with a diameter of 2.7 mm. The diameter of the region with CL coincided well with the diameter of the region with OH radicals above the solution surface. Since the image of the LIF intensity gives us a rough representation of the distribution of the OH radical density, the diameter of the region with OH radicals just above the liquid surface was approximately 2.6 mm. The diameter of the region with OH radicals was similar to the diameter of the region with CL.

Figure 5 shows temporal decays of the CL intensity (425 nm) and the optical emission intensity at the second positive band system of molecular nitrogen (337 nm), which were observed after the termination of the discharge current.

The inverted triangle plots indicate the decay of the OH LIF intensity just above the liquid surface. The optical emission intensity decayed rapidly after the termination of the discharge current. On the other hand, the CL intensity had a complicated waveform in the afterglow phase. We observed a rapid decay of the CL intensity immediately after the termination of the discharge current. The rapid decay was followed by a temporal increase, and after that, we observed a gradual decay of the CL intensity with a time constant of 100 μs. A similar temporal variation of the OH radical density has been reported by Verreycken and coworkers [26]. The decay of the OH LIF intensity had a similar temporal variation to the CL intensity as shown in figure 5.

4. Discussion

In a previous work [17], we reported that the CL spectrum induced by the plasma was different from that induced by the reaction with H_2O_2. The CL spectrum induced by the reaction with H_2O_2 had the peak at around 460 nm. However, we found in this work that the spectrum with the peak at around 460 nm was different from the true CL due to the absorption in the potassium ferricyanide solution. We measured the absorption spectrum of the potassium ferricyanide solution to reproduce the true CL spectrum induced by the reaction with H_2O_2. As a result, as shown in figure 2, it was found that the CL spectrum induced by the plasma was the same as that induced by the reaction with H_2O_2. A similar spectrum was observed by Xu and coworkers in the mixture of luminol and H_2O_2 in the presence of Cu nanoclusters as the catalyst [23]. According to Merenyi and coworkers, the CL spectrum with the peak at 425 nm is caused by the reaction between O_2^- and luminol [24, 25]. In the case of reaction with H_2O_2, O_2^- is produced by

$$Fe^{3+} + H_2O_2 \rightarrow Fe^{2+} + OOH + H^+ \quad (1)$$

and

$$OOH \leftrightarrow H^+ + O_2^-. \quad (2)$$

The same CL spectrum induced by the plasma irradiation indicates that the production pathway of O_2^-, which does not need the catalyst (Fe^{3+}), is available in the region just below the plasma-liquid interface.

The production process of O_2^- in the present experimental condition, where the liquid worked as the cathode of the discgarge, is not the direct transport from the gas phase. This is because O_2^- cannot pass through the potential barrier (on the order of 100 V) in the sheath above the liquid surface. It is reported that O_2^- is produced from OH radicals in the presence of H_2O_2 via the following reaction [25],

$$OH + H_2O_2 \rightarrow O_2^- + H_3O^+, \tag{3}$$

As shown in figure 3, we observed the correlation between the radial regions with CL and OH radicals in the gas phase. This correlation is reasonably understood by supposing the transport of gas-phase OH into the liquid side. Since it is sure that H_2O_2 is available in the liquid in the present experimental condition [27–29], OH radicals transported into the liquid are converted into O_2^- by reaction (3). The correlation between the decay waveforms of the luminol CL and the OH density in the afterglow phase, which are shown in figure 5, is also understood by the same manner. The disk shape of the CL intensity, which was observed when the distance between the needle electrode and the solution surface was 3 mm, is consistent with the distribution of the LIF image of OH above the solution surface, as shown in figure 4. On the other hand, we observed ring shapes of the CL intensity when the distance between the needle electrode and the solution surface was 1 mm. A probable mechanism for the ring CL intensity is the hollow distribution of the OH density just below the helium nozzle. The hollow distribution of the OH density just below the nozzle was observed in our previous work [8], where we reconstructed the accurate distribution of the OH density from the LIF image by considering the spatial distributions of the collisional quenching frequency and the rotational temperature. Another possible explanation for the ring CL intensity is the excess consumption of luminol by O_2^- at the central part.

As described above, the experimental results indicates that the radial distribution of the CL intensity represents the radial density distribution of liquid-phase OH radicals. In addition, the temporal variation of the liquid-phase OH radical density is represented by the temporal variation of the CL intensity. However, it is noted here that the depth profile of the CL intensity does not represent the depth profile of the O_2^- density in the liquid without the admixture of luminol. This is due to the high frequency for the reaction between O_2^- and luminol. The reaction rate coefficient for the reaction between O_2^- and luminol is 2.3×10^8 $M^{-1}s^{-1}$ [24], corresponding to a reaction frequency of 1×10^6 s^{-1} when the concentration of luminol is 5 mM. This means an efficient scavenging reaction of O_2^- by luminol, and the transport of O_2^- is prevented by this reaction. On the other hand, the rate coefficient for reaction (3) is 3.7×10^7 $M^{-1}s^{-1}$, corresponding to the reaction frequency of 1×10^7 s^{-1} if we assume a concentration of 1% for H_2O_2. The rate coefficient for the reaction between OH and luminol has not been reported, and is speculated to be much smaller than the rate coefficient for

reaction (3) [25]. Therefore, the admixture of luminol does not affect the density and its distribution of OH in the liquid. Since O_2^- produced from OH is scavenged by luminol efficiently, it is expected that the distribution of the CL intensity (or the blue disk) represents the distribution of the OH radical density in the liquid.

As described above, the present experimental results indicate that CL with a thin thickness is originated by the reaction between luminol and O_2^- which is produced by reaction (3). Note that the region with CL should be wider if O_2^- is produced from long-lived species. Another possible short-lived species which can produce O_2^- is solvated electron ($O_2 + e_{aq} \rightarrow O_2^-$). However, the lifetime of solvated electron is expected to be shorter than 1 μs [30], which contradicts the duration of CL in the afterglow (figure 5). Therefore, we believe that reaction (3) is a unique mechanism to explain the distribution and the duration of CL observed experimentally.

5. Conclusions

We investigated the correlation between the gas-phase OH density and the intensity of luminol CL in a liquid interacting with an atmospheric-pressure plasma. The luminol CL with a thin thickness was observed just below the plasma-liquid interface when the plasma was generated on the aqueous solution surface with luminol. The CL spectrum induced by the plasma irradiation indicates that the origin of CL is the reaction between O_2^- and luminol. We observed the spatiotemporal correlations between the CL intensity and the OH radical density in the gas phase. The correlation is reasonable since O_2^- is produced in the liquid by the reaction between H_2O_2 and OH transported from the gas phase. Since the density and its distribution of OH radicals is not affected by the admixture of luminol, we can conclude that the luminol CL reported in this paper is a useful method for the diagnostics of liquid-phase OH radicals induced by plasma-liquid interactions.

Acknowledgment

This work was supported by JSPS KAKENHI Grant Numbers 16H02121 and 18K03596. The authors thank Mr. Yutaka Matsuda of Hokkaido University for his help with the experimental assistant.

References

[1] P. Bruggeman and C. Leys: J. Phys. D **42** (2009) 053001.
[2] B. R. Locke, M. Sato, P. Sunka, M. R. Hoffman, and J. S. Chang: Ind. Eng. Chem. Res. **45** (2006) 882.
[3] P. Bruggeman et al: Plasma Sources Sci. Technol. **25** (2016) 053002.
[4] N. Shirai, K. Ichinose, S. Uchida, and F. Tochikubo: Plasma Sources Sci.Technol. **20** (2011) 034013.
[5] N. Shirai, M. Nakazawa, S. Ibula, amd S. Ishii: Jpn J. Appl. Phys. **48** (2009) 036002.
[6] N. Shirai, S. Uchida, and F. Tochikubo: Plasma Sources Sci. Technol. **23** (2014) 054010.

[7] K. Urabe, N. Shirai, K. Tomita, T. Akiyama and T. Murakami, Plasma Sources Sci. Technol. **25**(2016) 045004.
[8] H. Ishigame, S. Nishiyama, and K. Sasaki, Jpn J. Appl. Phys. **54** (2014) 01AF02.
[9] K. Sasaki, H. Ishigame, and S. Nishiyama, Eur. Phys. J. Appl. Phys. **71** (2015) 20807.
[10] N. Shirai, S. Uchida, and F. Tochikubo: Jpn. J. Appl. Phys. **53** (2014) 046202.
[11] N. Shirai, T. Yoshida, S. Uchida, and F. Tochikubo: Jpn. J. Appl. Phys. **56** (2017) 076201.
[12] E. Szili, J.-S. Oh, S.-H. Hong, A. Hatta, and R. D. Short: J. Phys. D: Appl. Phys. **48** (2015) 202001.
[13] D. Hayashi, W. Hoeben, G. Dooms, E. van Veldhuizen, W. Rutgers, and G. Kroesen: Appl. Opt. **40** (2011) 986.
[14] S. Kanazawa, H. Kawano, S. Watanabe, T. Furuki, S. Akamine, R. Ichiki, T. Ohkubo, M. Kocik and J. Mizeraczyk: Plasma Sources Sci. Technol. **20** (2011) 034010.
[15] K. Ninomiya, T. Ishijima, M. Imamura, T. Yamahara, H. Enomoto, K. Takahashi, Y. Tanaka, Y. Uesugi, and Nobuaki Shimizu: J. Phys. D. **46** (2013) 425401.
[16] F. Tochikubo, Y. Shimokawa, N. Shirai, S.Uchida: Jpn J. Appl. Phys. **53** (2014) 126201.
[17] N. Shirai, Y. Matsuda and K. Sasaki: Appl. Phys. Express **11** (2018) 016201.
[18] C. Lu, G. Song, J. Lin, *Trends in Anal. Chem.* **25** (2006) 985.
[19] M. J. Navas and A. M. Jimnez: Food Chem. **55** (1996) 7.
[20] A. W. Knight and G. M. Greenway: Analyst, **119** (1994) 879.
[21] F. Barni, S. W. Lewis, A. Bertia, G. M. Miskelly, G. Lagoa: Talanta **72** (2007) 896.
[22] P. B. Shevlin, H. A. Neufeld, *J. Org. Chem* **85** (1970) 2178.
[23] S. Xu, F. Chen, M. Deng, and Y. Sui: RSC Adv. **4** (2014) 15664.
[24] G. Merenyi, J. S. Lind and E. Erilsen: J. Biolumin. Chemilumin. textbf5 (1990) 53.
[25] G. Merenyi and J. S. Lind: J. Am. Chem. Soc. **102** (1980) 5830
[26] T. Verreycken, R. Horst, A. Baede, E. Veldhuizen and P. Bruggeman: J. Phys. D **45** (2012) 045205.
[27] S. Bekeschus, J. Kolata, C. Winterbourn, A. Kramer, R. Turner, K. Weltmann, B. Br ker and K. Masur: Free Radical Res. **48** (2014) 542549
[28] J Winter, H Tresp, M U Hammer, S Iseni, S Kupsch, A Schmidt-Bleker, K Wende, M Dnnbier, K Masur, K-D Weltmann: J. Phys. D. **47** (2014) 285401
[29] J. Liu, B. He, Q. Chen, J. Li, Q. Xiong, G. Yue, X. Zhang, S. Yang, H. Liu and Q. Liu: Sci. Rep. **6** (2016) 38454.
[30] G. V. Buxton, C. L. Greenstock, W. P. Helman and A. B. Ross: J. Phys. Chem. Ref. Data **17** (1988) 513.

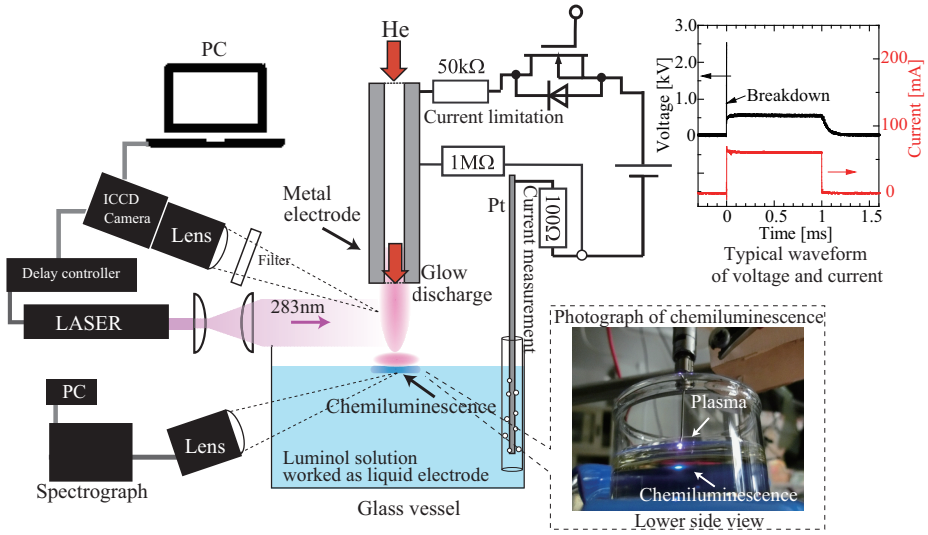

Figure 1. Schematic of the discharge system, the system for measuring the OH radical density in the gas phase, and the system for detecting the luminol CL in the liquid.

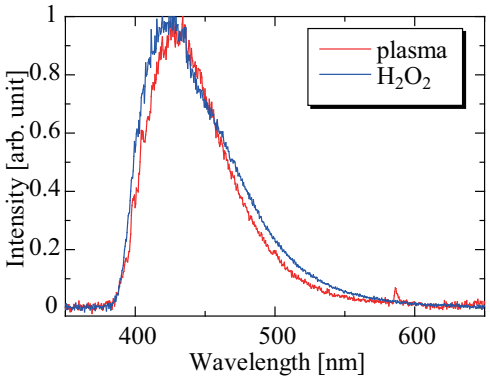

Figure 2. Spectrum of chemiluminescence induced by the plasma irradiation and by the reaction between H_2O_2 and luminol in the presence of Fe^{3+}

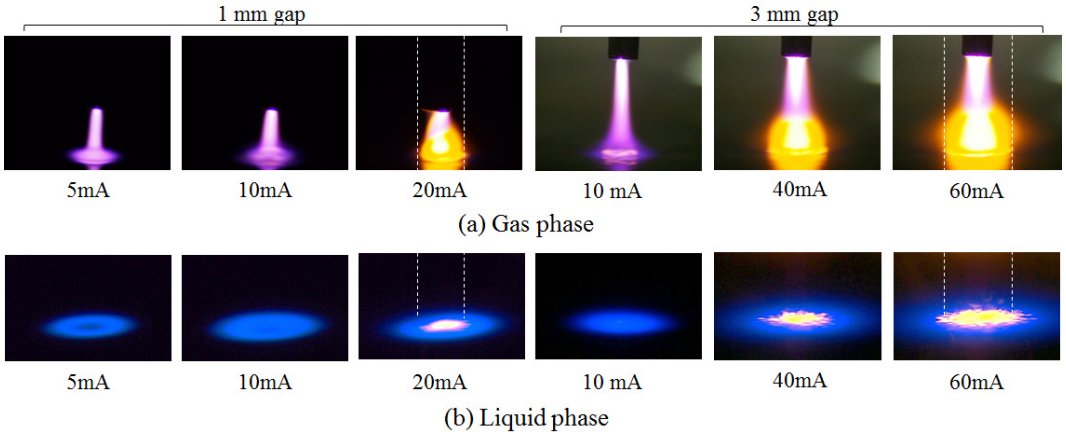

Figure 3. Photographs of the plasma and CL observed at various discharge currents. The liquid worked as the cathode and the distances between the tip of the nozzle electrode and the liquid surface were 1 and 3mm.

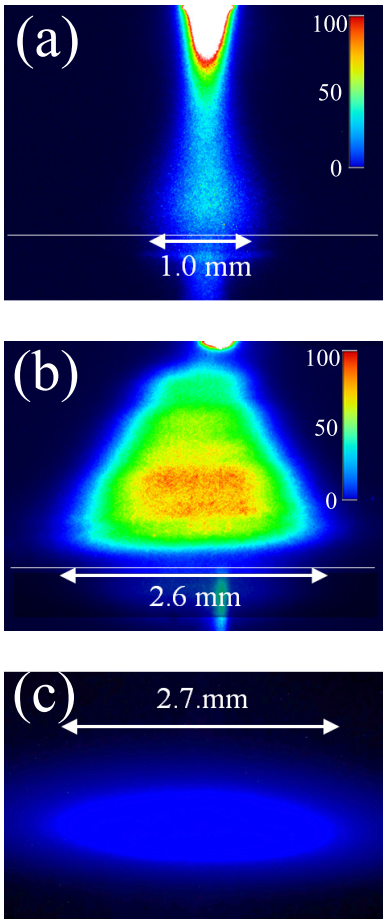

Figure 4. Comparison between the images of (a) the optical emission intensity of the plasma, (b) the LIF intensity of OH, and (c) the CL intensity. (c) was obtained by placing a blue filter which eliminated the optical emission of Na.

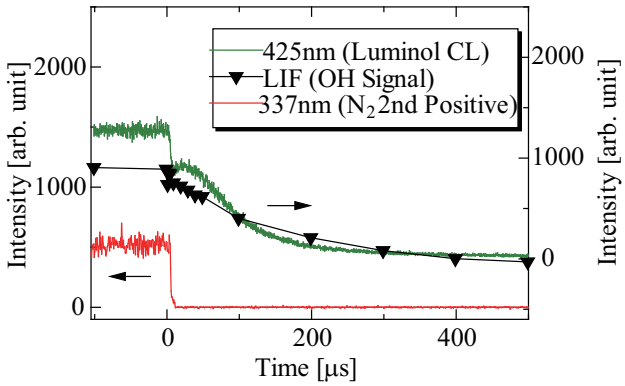

Figure 5. Temporal decays of the CL intensity and the optical emission intensity at the second positive band system of molecular nitrogen, which were observed after the termination of the discharge current. The concentration of luminol is 0.5 M.